

The 3D finite element analysis of stress distribution in implant supported single crown with different abutment designs

Pongsakorn Poovarodom¹⁾, Daraporn Sae- Lee¹⁾ and Jarupol Suriyawanakul²⁾

¹⁾Department of Prosthetic Dentistry, Faculty of Dentistry, Khon Kaen University, Khon Kaen 40002, Thailand

²⁾Department of Mechanical Engineering, Faculty of Engineering, Khon Kaen University, Khon Kaen 40002, Thailand

Received 4 July 2017
Accepted 22 September 2017

Abstract

At present, various implant abutments are available, but the effect of abutment design on the implant and surrounding bone of an implant supported single crown in the posterior region is limited. The purpose of this study was to investigate the maximum von Mises stress, stress distribution pattern and stress accumulation of implant supported by a single crown with various abutment designs in the posterior region.

A dental implant (4.5 mm in diameter and 11.5 mm in length), with three different implant abutments, i.e., Rigid, Transfer, and customized titanium abutments, with zirconia crowns, were modeled using geometric data in SolidWorks. ANSYS software was used for analysis of applied loads (200 N vertical and 40 N horizontal) at a functional area with 1 Hz for 5 seconds.

The results showed that the patterns of stress distribution in all models were similar, i.e., the maximum von Mises stresses were observed at the first thread of the implant fixture on the buccal side. In the bone, the maximum stress was observed at the marginal bone contact area with the first thread of the implant. The stress was concentrated at the implant fixture-abutment screw interface in the bottom area on the buccal side. The model with a customized abutment (model 3) had a lower maximum von Mises stress, compared with the prefabricated abutment models (models 1 and 2) in all components except the abutment.

A customized titanium abutment can provide better biomechanics than a prefabricated abutment. There is a lower maximum stress with a continuous stress distribution pattern, and the stress accumulation is less in the implant fixture. The stress in the abutment screw was distributed continuously with less stress concentration, and the stress is distributed uniformly to the bone with a low stress value.

Keywords: Finite element analysis, Dental implant, Abutment design, Customized abutment, Stress distribution

1. Introduction

Nowadays, implant supporting a single crown has become an optimal treatment for a single tooth replacement to restore the patient function, comfort and esthetics [1]. The success of implant treatment does not rely only on osseointegration, but it should be able to support a prosthesis function without pain, mobility or any signs and symptoms of local disease. Previous studies have demonstrated high survival rates of implants of a single tooth (>96.8%) and multiple teeth (>94%) [2-5]. Despite a high success rate in implant treatment, complications can still occur, e.g., peri-implantitis and soft tissue complications (9.7%), bone loss exceeding 2 mm (6.3%), implant fractures (0.14%), screw or abutment loosening (12.7%), screw or abutment fracture (0.35%) and ceramic or veneer fractures (4.5%) [5]. The common complications were related to the mechanical aspects [6]. According to the literature, implant failure was frequently induced by improper biomechanics of the dental implant, i.e., design and material of the abutment, unsuitable torque on the abutment screw when it is tightened into the

implant or stress distribution within the restoration [7]. Additionally, the occlusal force distribution is an important factor that can lead to implant failure, especially in the posterior region [8-10].

Improper biomechanics can occur in an early stage of treatment due to insufficient osseointegration between implant and surrounding bone. Then, the bone tissue could be replaced with fibrous connective tissue, so the implant cannot resist normal function forces [11]. Furthermore, implant failure can occur after insertion due to improper design of the implant fixture or abutment, i.e., the hole at the apical area of the implant fixture in the Zimmer® (Biomet 3i, USA) implant system, leading to a stress concentration in implant fixture and abutment. The smaller collar abutment in the SPI® (Alpha-Bio Tec, USA) implant system can increase the stress concentration in the cortical bone [12]. Thus, improper design may result in an overload of the abutment screw [7]. Micro-fractures at the bone-implant interface lead to implant failure [13]. Moreover, a general mechanical failure can also occur, i.e., fracture of the implant fixture,

abutment screws, bridge framework or ceramic coating of the restoration [11].

Bone is a self-adaptive material. In situations in which there is a change in the surrounding stress, the bone tissue structure can adapt by itself following the change of loading force. This phenomenon is called bone remodeling and it frequently occurs after the alteration of normal biological stress, which can lead to bone resorption. Meanwhile, implant supported restoration should be designed to transmit stress similar to the natural level through the tissue and surrounding bone. If the stress is greatly exceeded, it can induce osteoclast activities of the bone, which result in bone resorption and can lead to implant failures [14]. Furthermore, it will show unnatural phenomena with adjacent teeth, such as contact opening or spontaneous intrusion [15]. These may be due to the differences of stress distribution around the implant from adjacent teeth, since the periodontal ligament is lost after implant placement [14]. The long term effect of stress concentration at the implant and surrounding bone is still unclear. Therefore, it is important to verify this phenomenon to reduce undesirable stresses that occur in the bone. Hence, the biomechanics of dental implants has become an attractive area of research to improve the restoration methods for implant treatment.

From the problems above, several researchers have contributed to the developing of new abutment designs [16] to maintain good oral hygiene [17], optimize the load transfer from prosthesis to implant and surrounding bone [16], decrease abutment micro-movement and reduce stress concentration in the implant components [18]. A good candidate design to solve this problem is the custom abutment. It provides many advantages, e.g., optimal design of the crown contour, emergence profile and crown margin, and proper abutment design for individual patients [12]. Furthermore, it can reduce stress in implant components [19]. All of these factors can affect biomechanics.

However, there is an insufficient evidence base to address this issue and it is not easy to obtain a clinical or

laboratory study because of the limitation of patients, finance and methodology [20]. To study the effect of stress, the finite element method and parameterization optimum design techniques have been used extensively [21]. Studying stress concentration can be applied from a minimum to a maximum extent by performing multi-parameter optimization of the implant. Therefore, this method may provide more information on a proper dental implant component design that can distribute the occlusal load correctly to the surrounding bone to achieve the best biomechanics [7]. It can reduce the manufacturing costs over those incurred if each sample is actually built and tested [7, 21-22]. The aim of this study was to analyze the stress distribution in restorations supported by dental implants with various implant abutment designs in a mandibular first molar.

2. Materials and methods

2.1 Three dimesion (3D) model preparation

In this study, CAD models of implant components and related structures were created by SolidWorks (SolidWorks Version 2014, Dassault System, France). The OSSTEM™ implant series TS III (OSSTEM, Korea) was selected as a representative of a commercially available implant fixture and abutment design. The customized abutments were designed based on the Zirkonzhan system (Zirkonzahn, Italy). A summary of the CAD model is given in Table 1.

2.2 Finite element modeling

Three different models were used in the analysis related to the abutment models (Figure 1). Each model had five components, i.e., the abutment (Figure 1), crown, abutment screw, implant fixture and bone (cortical and cancellous), as shown in Figure 2. The abutment and screw were connected as one body, except in model 1, as shown in Figure 3.

Table 1 Components of the CAD model and their dimensions in the study.

Components	Details	Width (mm)	Length (mm)
Bone	Cortical bone	7.6	12.5
	Cancelloous bone	2 (thickness)	
Fixture	OSSTEM™ implant TS III	4.5	11.5
	Rigid abutment	4.5	11.5
Abutment	Transfer abutment	4.5	8.5
	Customized titanium abutment	7.6	10.5
Screw	Abutment screw	1.2	5
Crown	Zirconia crown		

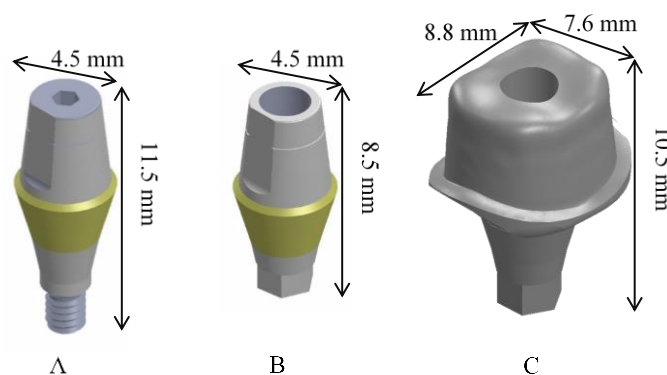


Figure 1 The abutment models in this study: (A) Rigid abutment, (B) Transfer abutment, (C) Customized titanium abutment.

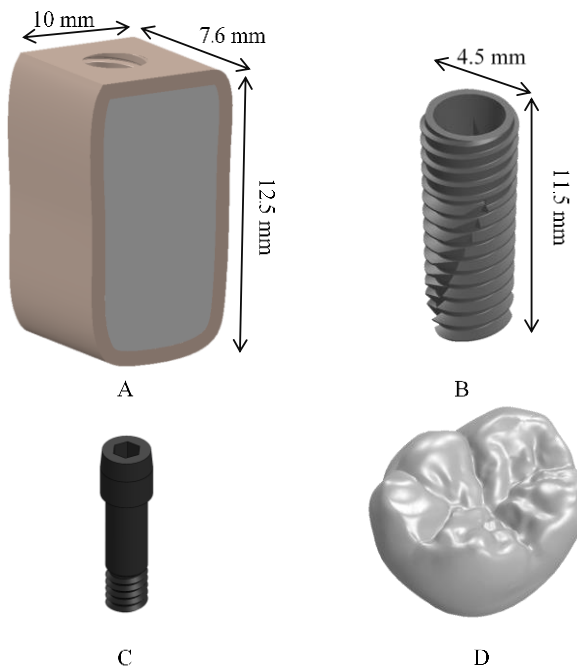


Figure 2 Component models in this study: (A) Cortical (brown) and Cancellous bone (gray), (B) Implant fixture, (C) Abutment screw and (D) Zirconia crown.

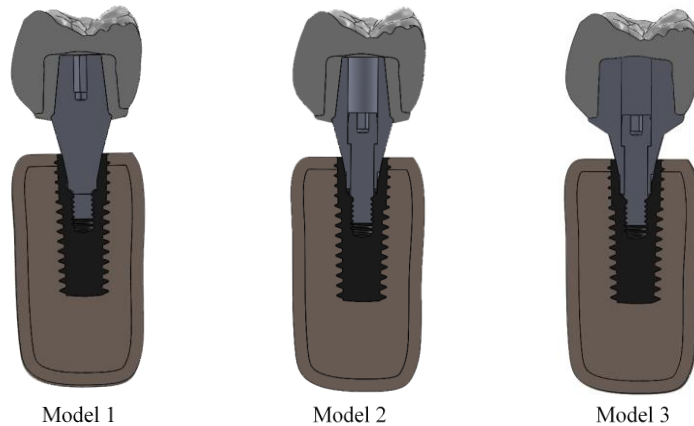


Figure 3 The crosssection view of 3D design models of bone (brown), implant (black), abutment screw (gray), titanium abutment (gray), zirconia crown (ivory) in each model.

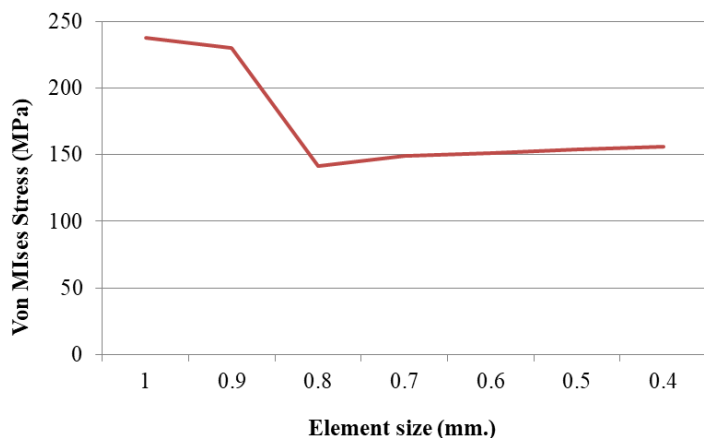


Figure 4 Mesh independence test graph.

Table 2 Material properties of implant fixture, implant abutment and crown materials.

Materials/ properties	Young's modulus (GPa)	Poisson's ratio	Yield Strength (MPa)
Titanium CP grade IV [23]	110	0.3	550
Zirconia (ZrO_2) [24]	200	0.35	1000

Table 3 Anisotropy elastic coefficients for cortical and cancellous bone.

Bone/properties	E_y	E_x	E_z	G_{yx}	G_{yz}	G_{xz}	ν_{yx}	ν_{yz}	ν_{xz}
Cortical [25]	12.7	17.9	22.8	5.0	7.4	5.5	0.18	0.28	0.31
Cancellous[26]	0.21	1.148	1.148	0.068	0.434	0.068	0.055	0.322	0.055

* E_i represents Young's modulus (GPa); G_{ij} represents shear modulus (GPa); ν_{ij} represents Poisson's ratio.

**The y-direction is infero-superior, the x-direction is medial-lateral, and the z-direction is anterior-posterior.

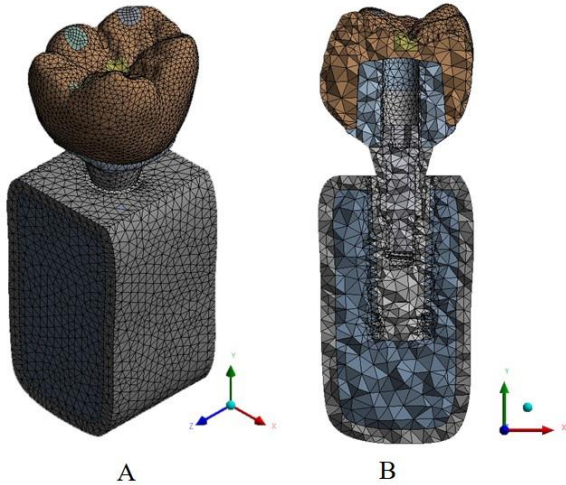


Figure 5 Model after the final meshing : (A) isometric view and (B) Crossection view.

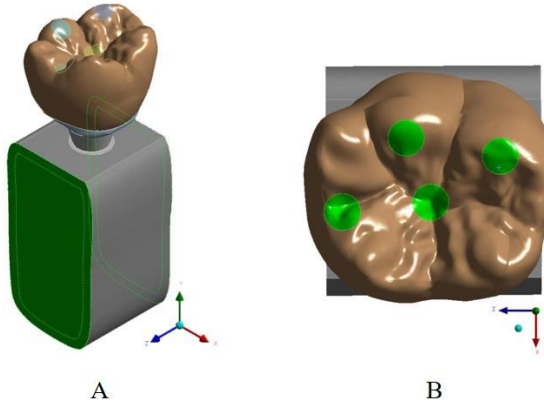


Figure 6 The boundary and loading conditions: (A) Fixed support area and (B) Loading area on functional cusp and groove.

2.3 Models meshing

The assembled models were transferred from SolidWorks to the ANSYS program (ANSYS Inc., USA). The specifications of mechanical properties of each model component were assigned (Table 2 and Table 3) and all components were assumed to be homogeneous with isotropic and linear elastic behavior, except bone was assumed as

anisotropic. After that, the mesh independence method was used and the result showed that the suitable element size was 0.6 mm. (Figure 4). The model was meshed with the tetrahedron method. The number of elements was approximately 100,000, with approximately 150,000 nodes. The meshed model is shown in Figure 5.

2.4 Boundary and loading conditions

A fixed support was selected at mesial and distal surfaces of the bone model, assuming no displacement in the x, y and z directions (Figure 6A). A quasi-static load was 200 N in the vertical (-Y) and 50 N in the horizontal (-X) direction [27-28] and was applied on a 4 functional loading area along the axis of the implant (Figure 6B) [29] at 1 Hz for 5 seconds (Figure 7). These estimations of 1 Hz were based on the assumption that an individual has three episodes of chewing per day, each 15 min in duration at a chewing rate of 60 cycles per minute (1 Hz). This is equivalent to 2700 chewing cycles per day or roughly 1,000,000 cycles per year [30]. In the literature, FEM implant studies often used a static analysis. However, in a real situation, teeth do not come into contact just one time (static). Rather, they are in contact with opposing teeth many times (dynamically) during chewing. Additionally, the dynamic load might be increased by 10-20% to the implant above the static loading, which may be the cause of fracture or fatigue failure of the prosthesis [31-32].

Moreover, nonlinear contact zones were defined at implant abutment, implant- screw and abutment- screw interfaces. Contact analysis assured the transfer of the load and deformation between the different components. The coefficient of friction was taken as 0.4 between all the titanium-titanium interfaces [33]. However, in this study, it was assumed that the contact between thread of the abutment screw and thread of the implant screw hole was completely seated and was not permitted to shift or displace, hence the effect of screw movement was excluded in this study. A bond contact was applied between the crown and the abutment in all models. As shown in a previous FEM study, the effect of the cement layer on the stress distribution was negligible [34]. The bone-implant interface was assumed to be fully osseointegrated. The components in the model were all assumed to be homogeneous and isotropic. They were also linearly elastic, except bone. It was assumed to be anisotropic according to the material properties from studies by Schwartz-Dabney in 2003 [25] and O'Mahony in 2000 [26]. These were inherent limitations of this study.

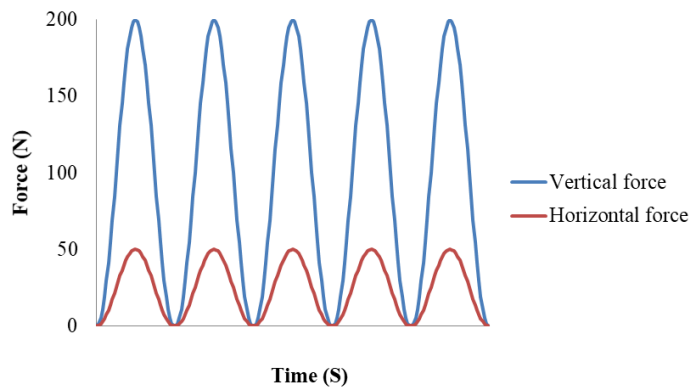


Figure 7 Magnitude of loading force in five seconds, both vertically (blue) and horizontally (red).

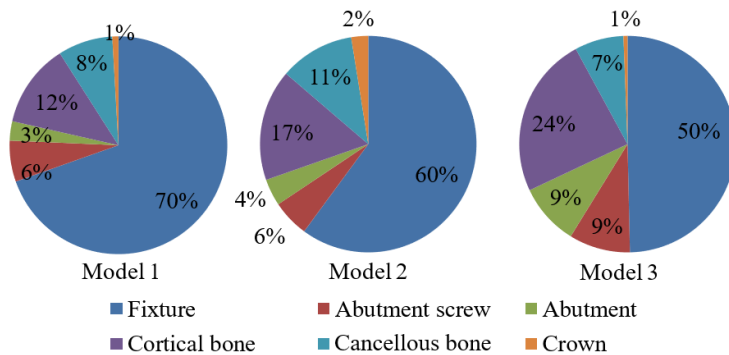


Figure 8 The von Mises stress accumulation in various components of each model.

2.5 The Results interpretation

As the numerical values gained from stress analysis are mathematical calculations without variance, statistical analyses were not required as in a routine procedure for a conclusion. However, an interpretation of stress analysis results for clinical applications is necessary. Nevertheless, there are no explicit guidelines in the literature, or any suggestions regarding the kind of stresses that must be used in the explanation. This study focused on the stress distribution pattern in the implant components through the bone. Therefore, von Mises stress was used for result interpretation.

3. Results

3.1 The von Mises stress accumulation

According to the literature, results have been interpreted in two common ways, maximum stress and stress distribution. Nevertheless, the maximum stress could be in error by improper modeling (an edge, ledge, or gap in the model), improper meshing, and errors in processing. Moreover, the stress distribution was shown in color patterns and described in 2D, which explained behavior of stress distribution area in two directions. Only two aspects of results do not satisfactorily address the biomechanics in dental implants. Therefore, Von Mises stress accumulation was used to explain the stress transmutation in the model and stress accumulation in each component. The stress transmutation represents force transmission, gives information to explain the biomechanics in dental implants.

The stress values of every element of all models were exported. Then all stress values in each component were computed as a percentage of total stress in that model. This is presented as a pie graph to show the trends of stress accumulation in the models (Figure 8). The von Mises stress accumulation in every model primarily accumulated at the implant fixture and cortical bone. The highest cumulative stress of implant fixture was observed in model 1 (69.59 %), and the lowest cumulative stress was observed in model 3 (50 %). In the customized abutment (model 3), the stress was accumulated less in the fixture and cancellous bone than in other models. Rather, the stress was accumulated more in the cortical bone, abutment and abutment screw than in other models.

3.2 The maximum von Mises stress

In this study, the normal stress value in each axis was less than the tensile strength and compressive strength of the abutment material. Thus, no components in this study fractured.

The maximum values of stress in each model are shown in Figures 9 and 10. The results showed that the patterns of stress distribution in all models were similar (Figure 11). The highest maximum stress was observed at the first thread of the implant fixture on the buccal side. In the cortical bone, the maximum stress was observed at the marginal bone contact area with the first thread of the implant. Furthermore the stress was concentrated at the implant fixture-abutment screw interface in the bottom area at the buccal side. The model with a customized abutment (model 3) had a lower maximum von Mises stress compared to the implants with prefabricated abutments (models 1 and 2) in all components except in the abutment.

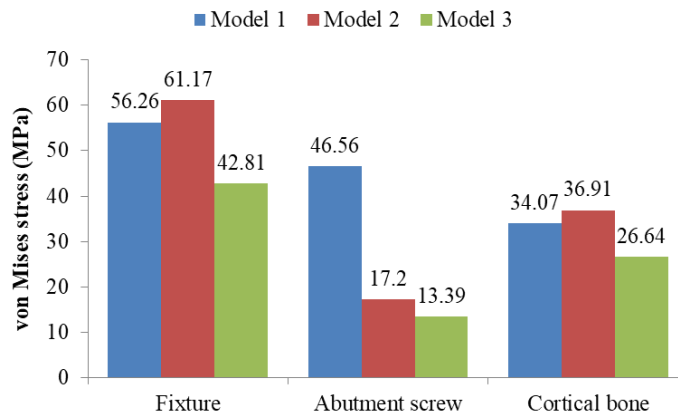


Figure 9 Histogram of the maximal von Mises stresses in the fixture, abutment screw and cortical bone components.

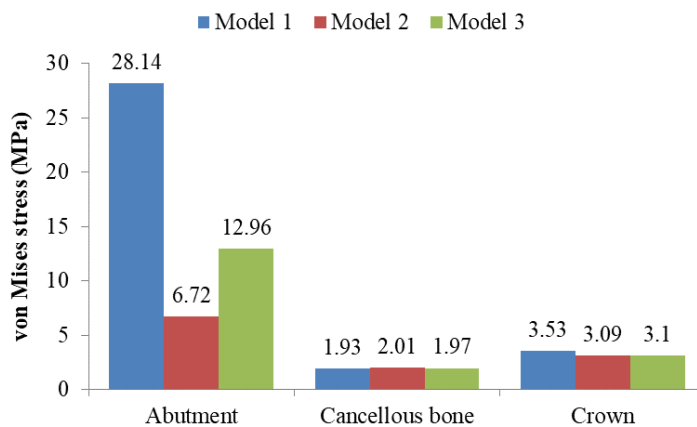


Figure 10 Histogram of the maximal von Mises stresses in the abutment, cancellous bone and crown components.

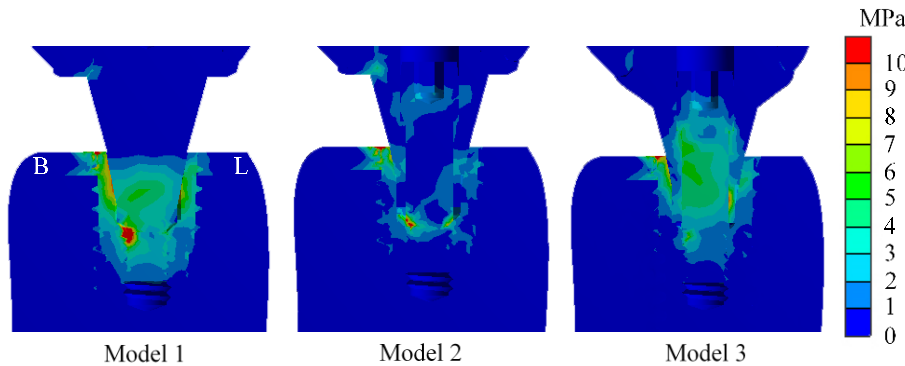


Figure 11 The von Mises stress distributions of all models in buccolingual cross-sectional images.

3.3 The von Mises stress distribution of each component

The stress distribution in the cortical bone (Figure 12) was predominantly concentrated around the bone-implant contact interface area. In the occlusal view, a high stress concentration was observed on the buccal and distal side. Moreover in the buccolingual cross-sectional view, the stress was concentrated more on the buccal side than on the lingual.

The stress distribution in the cancellous bone (Figure 13) was observed at the bone-implant contact interface. Stress was concentrated more on the buccal side than on the lingual. In the stress distribution pattern of model 2, stress was concentrated more on the buccal side to a greater degree than in other models, and in model 1, stress was concentrated more on the lingual side than in other models.

The stress distribution in the fixture (Figure 14) in the buccal view, a high stress concentration (red) was observed in zone A of the implant (1st and 2nd thread). In model 2, the stress distribution was restricted to zone B with a discontinuous pattern. Model 1 showed a continuous stress distribution to zone D. The stress distribution pattern, in the model with a customized abutment (model 3), was continuously distributed to zone C. In the buccolingual cross-sectional view, a high stress concentration was observed at the implant-abutment connection and the thread of the screw hole. The model with a customized abutment (model 3) had a lower stress concentration than the models with prefabricated abutments (models 1 and 2), especially at the thread of the screw hole. Model 1 demonstrated the largest stress concentration area (zones A and B), but the

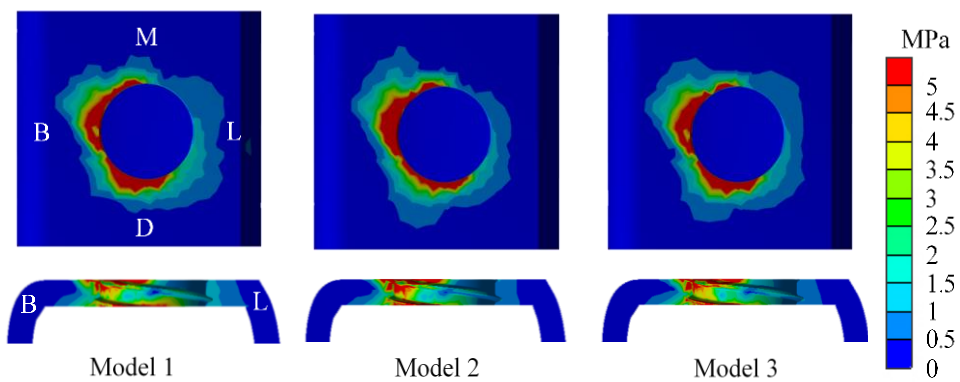


Figure 12 The von Mises stress distribution at the cortical bone in an occlusal view (upper) and buccolingual cross-sectional view (lower).

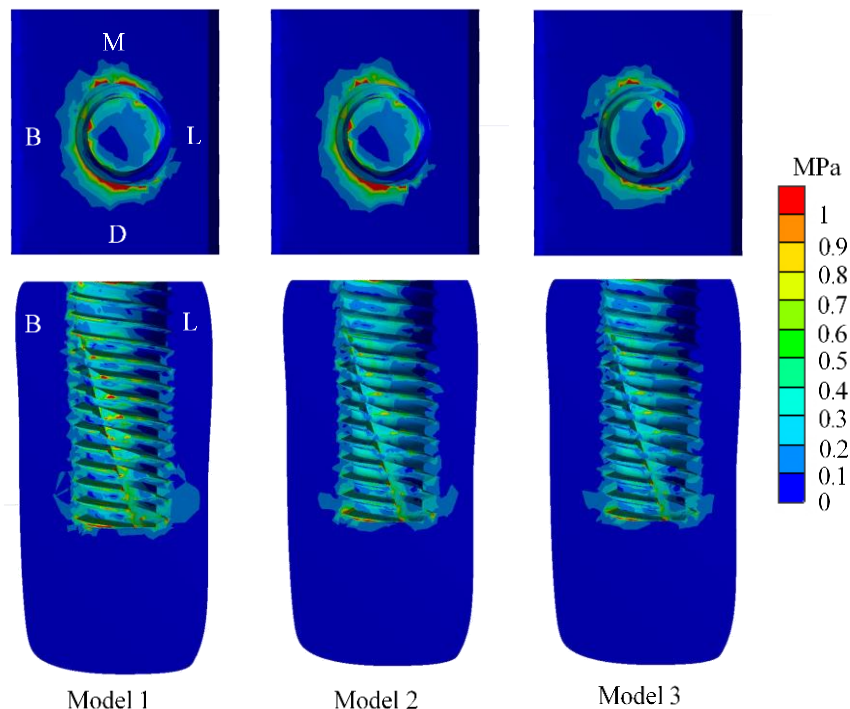


Figure 13 The von Mises stress distribution in the cancellous bone in an occlusal view (upper) and buccolingual cross-sectional view (lower).

stress could be distributed to zone C. In model 2, the stress was restricted to zone B in a discontinuous pattern.

The stress distribution in the abutment screw (Figure 15), in the buccal view the stress concentration was observed at the middle portion and at the threads of the abutment screw. A high stress concentration in the model with a customized abutment (model 3) was less than the models with prefabricated abutments (models 1 and 2), especially at the threads of the screw. In the buccolingual cross-sectional view, a high stress concentration was observed in the middle portion and at the threads of the abutment screw. The stress was concentrated at the buccal side more than on the lingual side. The stress distribution in the model with a customized abutment (model 3) was distributed continuously along the screw. In the prefabricated models, model 1 showed the highest stress concentration. In model 2, the stress was restricted to the upper part of the screw in a discontinuous pattern.

In the buccal view of the stress distribution in the abutment (Figure 16), the stress concentration was observed at the conical and hexagonal surface of the internal connection. The model with a customized abutment (model 3) had a lower stress concentration than the models with prefabricated abutments (models 1 and 2), especially at the hexagonal surface. The stress distribution in the model with a customized abutment (model 3) was distributed continuously along the conical and hexagon surfaces. In the prefabricated models, model 1 showed the highest stress concentration, especially at the abutment-screw connection. In model 2, stress was restricted to the upper part of the abutment in a discontinuous pattern.

The stress distribution in the crown (Figure 17) was observed at the crown margin. In the customized abutment (model 3), stress was concentrated on the buccal and lingual sides, whereas in the prefabricated models (models 1 and 2) the stress was concentrated only on the buccal side.

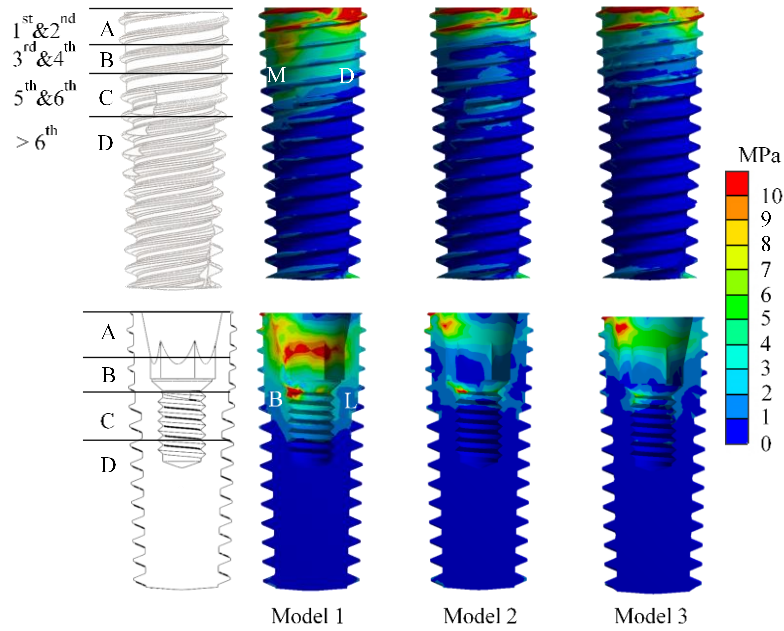


Figure 14 The von Mises stress distribution of fixture in buccal view (upper) and buccolingual cross-sectional view (lower).

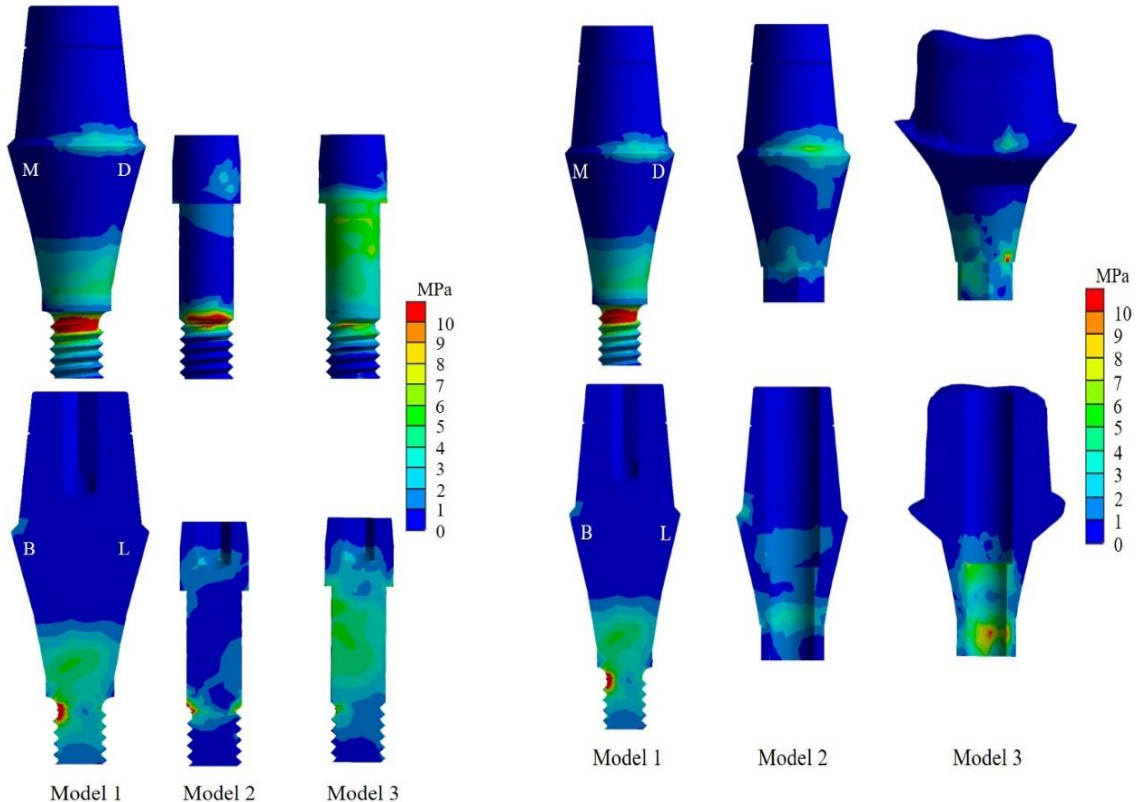


Figure 15 The von Mises stress distribution of abutment screw in buccal (upper) and buccolingual cross-sectional (lower) views.

4. Discussion

Loading conditions are an important consideration in FEM. In the current study, a combined load (vertical and horizontal) was used. This load was used as it is more realistic than using only a vertical load [35]. A non-axial load

Figure 16 The von Mises stress distribution of abutment in buccal view (upper) and buccolingual crosssection view (lower).

will create tensile stress and a bending movement was applied to each component. This can lead to the destruction of an implant, connection components or peri-implant bone [36]. The loading area is also affected. Several studies used a cusp-to-fossa relationship with maximal intercuspalation with no eccentric or interceptive occlusal contacts. Furthermore when occlusal force occurs during

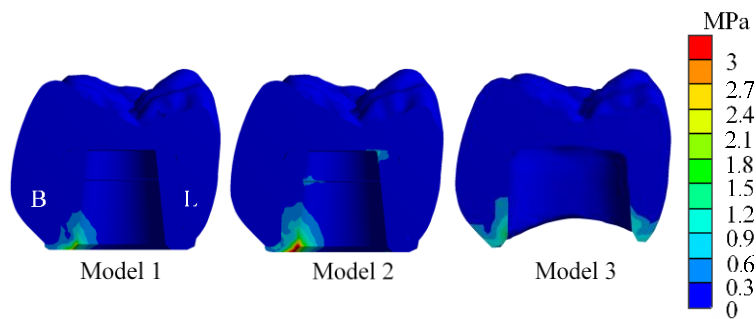


Figure 17 The von Mises stress distribution in a crown in buccal view (upper).

chewing, it transmits through the functional cusps that contact with the fossa of the opposing tooth to the implant component. However, occlusion of the dental implant was usually developed with a protected occlusion [37], in which the contact area at functional cusps is absent. This study considered a worst case scenario in which the load was applied in a group function occlusion. Hence, the loading was applied to the functional area of the anatomical crown, and these areas were selected in this study. This is more reasonable and clinically relevant than applying it directly to the abutment [22, 38]. Thus, in the current study, a 200 N vertical load [27], combined with a 50 N horizontal load [39–40] was applied to the function cusps and fossa of an anatomical crown that simulates a chewing force in the oblique direction.

In the present study, stress was concentrated more on the buccal side than the lingual side of the implant-abutment complex. This resulted in a slight displacement of the crown in the buccal direction. Sakaguchi and Borgersen, in 1993, reported the separation between a gold screw and the crown was related to a high stress concentration on the buccal portion compared to the lingual portion of the abutment-implant complex [41]. Cehreli et al., in 2004, also reported horizontal implant displacement resulting from application of vertical or oblique loads [42]. The separation between the crown, abutment, and screw had arisen from micro-movement of the implant system. If this deformation occurred, it could result in a fracture or loosening of the abutment screws [42] and bone loss around the implant [43]. They concluded that linear elastic analysis does not simulate the contact behavior that results in increasing stress distributions in regions where clinical failures usually occur [41]. The clinical behavior of implant components must be considered in non-linear analysis. Previous studies used linear elastic analysis, which does not allow for plastic deformation or separation at the contact area. Contact analysis demonstrates separations at the crown-abutment interface and crown-retaining screw interface, which are consistent with those found in an *in vitro* simulation in a servohydraulic robotic testing instrument [44]. A non-linear contact analysis would be a more realistic method to simulate the micro-motions that can potentially occur between the components with a frictional coefficient used to define the interfacial conditions [21].

In this study, the stress was concentrated at the abutment-implant complex in all models, especially on the abutment screw, which may be related to frequent complications. Corresponding to the systematic review of the complications by Jung et al. in 2008, failures included screw or abutment loosening (12.7%), screw fracture (0.35%) and bone loss exceeding 2 mm (6.3%) [5]. The incidence of bone loss conformed to the maximum von Mises stress in this study,

stress concentrated around the implant thread, especially the upper portion of the implant, i.e., the first and second threads of the implant. This could be related to cortical bone resorption around the implant.

The maximum von Mises stress in the cortical bone was found in model 2 (36.91 MPa). The stresses which occurred under the conditions of this study (model, loading conditions and material properties) were lower than the ultimate tensile and compressive strength of cortical bone. The ultimate tensile and compressive strength values for cortical bone are 121 MPa and 167 MPa, respectively [45]. Hassler et al. [46] in 1980 evaluated bone remodeling in rabbit calvarium with strain gauges and FEM. They reported that bone formation is positive for compressive stresses between 0 and 360 psi (0 to 2.48 MPa). At stresses above 400 psi (2.75 MPa), little or no bone formation occurs, but destruction of bone is not seen until the stress levels approach 1,000 psi (6.9 MPa). The values obtained in cortical bone in the present study were higher than those of Hassler et al. This variation may originate from the differences between the elastic moduli of cortical bone (defined as 17.9 GPa) and rabbit calvarium (defined as 0.689 GPa). The elastic modulus of rabbit calvarium is approximately 20 times lower than the elastic modulus of human cortical bone. Differences in the direction and amount of loading may also affect the modulus of elasticity.

In this study, the comparison between models with prefabricated abutments (models 1 and 2) and a model with a customized abutment (model 3) exhibited similar trends for maximum stress and stress distribution (Figure 11). The model with a customized abutment had a lower maximum stress with continuous stress distribution patterns. The stress was less in the implant fixture. In the abutment screw, the stress was distributed continuously and there was less stress concentration. The stress was distributed to the bone at a low level. This is because the customized abutment has a collar on the abutment that is bigger than the prefabricated abutment. The larger collar can distribute stress better. This is in agreement with Mammadzada et al. (2011). They concluded that the shape of the abutment had a direct relationship to the stress distribution on the abutment, implant fixture and bone [12]. This trend can indicate that the model with a customized abutment can provide better biomechanics for implant supported single crown restoration, in agreement with Kim et al. (2013), who compared various abutment types using FEM and an *in vitro* study (Transfer, Custom Fit™, ZioCera and MYPLANT Zirconia Hybrid abutments). The results showed that using a customized abutment can improve the fracture resistance of a restoration [47]. A retrospective study by Korsch (2015) revealed that a customized abutment had an incidence of screw loosening of 3.1% (3 from 96 total), whereas

prefabricated abutments loosened at a rate of around 8% (25 from 312 total). They concluded that the use of a customized abutment can reduce screw loosening in implant supported single crown restorations. However, this study reported the incidence in the anterior region [48].

In a natural tooth, it is obvious that chewing force distributes continuously through the surrounding bone along the periodontal ligament [45]. Thus the biomechanics of dental implants should present similar behavior. A dental implant system should be able to distribute stress into the bone in a continuous pattern. In the present study, the customized abutment model (model 3) exhibited a continuous stress distribution pattern with low stress in the surrounding bone.

5. Conclusions

The results showed that a customized abutment can provide better biomechanics than a prefabricated one. There was a lower maximum stress with a continuous stress distribution pattern, and a lower stress accumulation in the implant fixture. The stress in the abutment screw was distributed continuously with less stress concentration, and the stress was distributed and accumulated to the bone at lower levels. The von Mises stress accumulation provides a new aspect of stress analysis in FEM.

In future, more laboratory tests and clinical trials are necessary to further confirm the findings of the present study, i.e., the optimization of abutment design, the effect of screws, the torque removal from the retention screw and long term follow up in patients.

6. Acknowledgements

The researchers would like to express their sincere thanks to the Faculty of Dentistry, Khon Kaen University for the supportive research funding. Additionally, we are grateful for the advice of colleagues in the Research Unit on Mechanical Component Design, Mechanical Engineering Department, Faculty of Engineering, Khon Kaen University and for the SolidWorks software and ANSYS software license.

7. References

- [1] Jivraj S, Chee W. Treatment planning of implants in the aesthetic zone. *Br Dent J.* 2006;201(2):77-89.
- [2] Creugers NH, Kreulen CM, Snoek PA, de Kanter RJ. A systematic review of single-tooth restorations supported by implants. *J Dent.* 2000;28(4):209-17.
- [3] Jemt T, Lekholm U. Oral implant treatment in posterior partially edentulous jaws: a 5-year follow-up report. *Int J Oral Maxillofac Implants.* 1993;8(6):635-40.
- [4] Eckert SE, Wollan PC. Retrospective review of 1170 endosseous implants placed in partially edentulous jaws. *J Prosthet Dent.* 1998;79(4):415-21.
- [5] Jung RE, Pjetursson BE, Glauser R, Zembic A, Zwahlen M, Lang NP. A systematic review of the 5-year survival and complication rates of implant-supported single crowns. *Clin Oral Implants Res.* 2008;19(2):119-30.
- [6] el Askary AS, Meffert RM, Griffin T. Why do dental implants fail? Part I. *Implant Dent.* 1999;8(2):173-85.
- [7] Van Staden RC, Guan H, Loo YC. Application of the finite element method in dental implant research. *Comput Methods Biomed Engin.* 2006;9(4):257-70.
- [8] Isidor F. Loss of osseointegration caused by occlusal load of oral implants. A clinical and radiographic study in monkeys. *Clin Oral Implants Res.* 1996;7(2):143-52.
- [9] Isidor F. Influence of forces on peri-implant bone. *Clin Oral Implants Res.* 2006;17(Suppl 2):8-18.
- [10] Lops D, Bressan E, Chiapasco M, Rossi A, Romeo E. Zirconia and titanium implant abutments for single-tooth implant prostheses after 5 years of function in posterior regions. *Int J Oral Maxillofac Implants.* 2013;28(1):281-7.
- [11] Esposito M, Hirsch JM, Lekholm U, Thomsen P. Biological factors contributing to failures of osseointegrated oral implants. (I). Success criteria and epidemiology. *Eur J Oral Sci.* 1998;106(1):527-51.
- [12] Mammadzada S, Artunç C, Sen F, Güngör MA, Tekin U, Çömlekoglu E. Effect of abutment and implant shapes on stresses in dental applications using fem. *Math Comput Appl.* 2011;16(2):546-55.
- [13] el Askary AS, Meffert RM, Griffin T. Why do dental implants fail? Part II. *Implant Dent.* 1999;8(3):265-77.
- [14] VanSchoiack LR, Wu JC, Sheets CG, Earthman JC. Effect of bone density on the damping behavior of dental implants: an in vitro method. *Mater Sci Eng C.* 2005;26(8):1307-11.
- [15] Sheets CG, Earthman JC. Tooth intrusion in implant-assisted prostheses. *J Prosthet Dent.* 1997;77(1):39-45.
- [16] Bozkaya D, Muftu S, Muftu A. Evaluation of load transfer characteristics of five different implants in compact bone at different load levels by finite elements analysis. *J Prosthet Dent.* 2004;92(6):523-30.
- [17] Taiyeb-Ali TB, Toh CG, Siar CH, Seiz D, Ong ST. Influence of abutment design on clinical status of peri-implant tissues. *Implant Dent.* 2009;18(5):438-46.
- [18] Yamanishi Y, Yamaguchi S, Imazato S, Nakano T, Yatani H. Effects of the implant design on peri-implant bone stress and abutment micromovement: three-dimensional finite element analysis of original computer-aided design models. *J Periodontol.* 2014;85(9):e333-8.
- [19] Wu T, Liao W, Dai N, Tang C. Design of a custom angled abutment for dental implants using computer-aided design and nonlinear finite element analysis. *J Biomech.* 2010;43(10):1941-6.
- [20] Nothdurft F, Pospiach P. Prefabricated zirconium dioxide implant abutments for single-tooth replacement in the posterior region: evaluation of peri-implant tissues and superstructures after 12 months of function. *Clin Oral Implants Res.* 2010;21(8):857-65.
- [21] Geng JP, Tan KB, Liu GR. Application of finite element analysis in implant dentistry: a review of the literature. *J Prosthet Dent.* 2001;85(6):585-98.
- [22] Hsu M-L, Chang C-L. Application of Finite Element Analysis in Dentistry. In: Moratal D, editor. *Finite Element Analysis.* Croatia: InTech; 2010. p. 43-55.
- [23] Pierrisnard L, Hure G, Barquins M, Chappard D. Two dental implants designed for immediate loading: a finite element analysis. *Int J Oral Maxillofac Implants.* 2002;17(3):353-62.
- [24] Kohal RJ, Papavasiliou G, Kamposiora P, Tripodakis A, Strub JR. Three-dimensional computerized stress analysis of commercially pure titanium and yttrium-partially stabilized zirconia implants. *Int J Prosthodont.* 2002;15(2):189-94.
- [25] Schwartz-Dabney CL, Dechow PC. Variations in cortical material properties throughout the human

dentate mandible. *Am J Phys Anthropol.* 2003;120(3):252-77.

[26] O'Mahony AM, Williams JL, Katz JO, Spencer P. Anisotropic elastic properties of cancellous bone from a human edentulous mandible. *Clin Oral Implants Res.* 2000;11(5):415-21.

[27] Mericske-Stern R, Assal P, Mericske E, Burgin W. Occlusal force and oral tactile sensibility measured in partially edentulous patients with ITI implants. *Int J Oral Maxillofac Implants.* 1995;10(3):345-53.

[28] Weinstein AM, Klawitter JJ, Anand SC, Schuessler R. Stress analysis of porous rooted dental implants. *J Dent Res.* 1976;55(5):772-7.

[29] Saidin S, Abdul Kadir MR, Sulaiman E, Abu Kasim NH. Effects of different implant-abutment connections on micromotion and stress distribution: prediction of microgap formation. *J Dent.* 2012;40(6):467-74.

[30] Wiskott HW, Nicholls JI, Belser UC. Stress fatigue: basic principles and prosthodontic implications. *Int J Prosthodont.* 1995;8(2):105-16.

[31] Binon PP, McHugh MJ. The effect of eliminating implant/abutment rotational misfit on screw joint stability. *Int J Prosthodont.* 1996;9(6):511-9.

[32] JK Z, ZQ C. The study of effects of changes of the elastic modulus of the materials substitute to human hard tissues on the mechanical state in the implant-bone interface by three-dimensional anisotropic finite element analysis. *West China J Stomatol.* 1998;16:274-8.

[33] Alkan I, Sertgoz A, Ekici B. Influence of occlusal forces on stress distribution in preloaded dental implant screws. *J Prosthet Dent.* 2004;91(4):319-25.

[34] Toksavul S, Zor M, Toman M, Gunor MA, Nergiz I, Artunc C. Analysis of dentinal stress distribution of maxillary central incisors subjected to various post-and-core applications. *Operat Dent.* 2006;31(1):89-96.

[35] Chun HJ, Cheong SY, Han JH, Heo SJ, Chung JP, Rhyu IC, et al. Evaluation of design parameters of osseointegrated dental implants using finite element analysis. *J Oral Rehabil.* 2002;29(6):565-74.

[36] Barbier L, Vander Sloten J, Krzesinski G, Schepers E, Van der Perre G. Finite element analysis of non-axial versus axial loading of oral implants in the mandible of the dog. *J Oral Rehabil.* 1998;25(11):847-58.

[37] Misch CE, Bides MW. Implant-protected occlusion. *Int J Dent Symp.* 1994;2(1):32-7.

[38] Alvarez-Arenal A, Segura-Mori L, Gonzalez-Gonzalez I, Gago A. Stress distribution in the abutment and retention screw of a single implant supporting a prosthesis with platform switching. *Int J Oral Maxillofac Implants.* 2013;28(3):e112-21.

[39] Tada S, Stegaroiu R, Kitamura E, Miyakawa O, Kusakari H. Influence of implant design and bone quality on stress/strain distribution in bone around implants: a 3-dimensional finite element analysis. *Int J Oral Maxillofac Implants.* 2003;18(3):357-68.

[40] Canay S, Hersek N, Akpinar I, Asik Z. Comparison of stress distribution around vertical and angled implants with finite-element analysis. *Quintessence Int.* 1996;27(9):591-8.

[41] Sakaguchi RL, Borgersen SE. Nonlinear finite element contact analysis of dental implant components. *Int J Oral Maxillofac Implants.* 1993;8(6):655-61.

[42] Cehreli MC, Akca K, Iplikcioglu H. Force transmission of one- and two-piece morse-taper oral implants: a nonlinear finite element analysis. *Clin Oral Implants Res.* 2004;15(4):481-9.

[43] Hermann JS, Schoolfield JD, Schenk RK, Buser D, Cochran DL. Influence of the size of the microgap on crestal bone changes around titanium implants. A histometric evaluation of unloaded non-submerged implants in the canine mandible. *J Periodontol.* 2001;72(10):1372-83.

[44] DeLong R, Douglas WH. An artificial oral environment for testing dental materials. *IEEE Trans Biomed Eng.* 1991;38(4):339-45.

[45] Akca K, Iplikcioglu H. Evaluation of the effect of the residual bone angulation on implant-supported fixed prosthesis in mandibular posterior edentulism. Part II: 3-D finite element stress analysis. *Implant Dent.* 2001;10(4):238-45.

[46] Hassler CR, Rybicki EF, Cummings KD, Clark LC. Quantification of bone stresses during remodeling. *J Biomech.* 1980;13(2):185-90.

[47] Kim H-E, Cho I-H. Stress Analysis and Fatigue Failure of Prefabricated and Customized Abutments of Dental Implants. *J Dent Rehabil Appl Sci.* 2013;29(3):209-23.

[48] Korsch M, Walther W. Prefabricated Versus Customized Abutments: A Retrospective Analysis of Loosening of Cement-Retained Fixed Implant-Supported Reconstructions. *Int J Prosthodont.* 2015;28(5):522-6.